IL NUOVO CIMENTO Vol. 24 C, N. 6 Novembre-Dicembre 2001

Regimes in moist stratified flows over isolated topography: Numerical experiments

M. M. Miglietta(*) and A. Buzzi

Istituto di Scienze dell'Atmosfera e dell'Oceano, ISAO-CNR - Via Gobetti 101, Bologna, Italy

(ricevuto il 7 Settembre 2000; revisionato il 2 Gennaio 2001; approvato il 23 Gennaio 2001)

Summary. — Moist flows over simply shaped 3D mountains have been studied in numerical simulations made with a mesoscale meteorological model. Our aim is to examine the possible existence of multiple solutions, searching for different solutions depending on the path followed by the system in the parameter space. Results from three different sets of experiments are discussed here. In the first set of simulations, the height of the mountain has been progressively changed in time. In the second group of experiments, the humidity of the air flowing over the obstacle has been increased in time by adding a source term to the equation of evolution of moisture. The case of advection of moist air towards an obstacle, initially embedded in dry air, has been studied as a third type of flow. A dependence on the past history of the flow seems to characterise some types of system evolution, leading to different flow regimes over the obstacle. The experiments indicate that this result is mainly a consequence of changes of state of water, associated with the presence of humidity in the atmosphere. These effects are emphasised in the case of an elliptical mountain, with its longer axis perpendicular to the main flow. In the three different sets of experiments presented here, evident differences with simulations where flow parameters are kept constant from the beginning persist in the flow regimes, also for periods of time much longer than the characteristic time of evolution towards stationary solutions.

PACS 92.60.Jq – Water in the atmosphere (humidity, clouds, evaporation, precipitation).
PACS 92.60 – Meteorology.

1. – Introduction

The effect of simply shaped 3D mountains on dry, inviscid, non-rotating flows has been already analysed in several studies, mainly based on results of numerical experiments (see, for example [1-3]). The effects of humidity and condensation on flow patterns, however,

(*) Present affiliation: Ufficio Generale di Meteorologia, Roma, Italy.

have received so far comparatively little attention in the literature. Actually, earlier studies have shown that flow dynamics can be effectively modified by the presence of regions where condensation occurs [4, 5]. Only very recently, the study of the effect of moisture over 3D idealised stratified flows has been undertaken in a more systematic way, in the case of simply shaped mountains and simple upstream flows [6-8].

The analysis of numerical simulations of events of orographic precipitation [9] has shown that the presence of moisture can determine the characteristics of the flow regime in upstream and near-orography regions, by effectively changing the flow with respect to the dry case with the same upstream profiles. This result can be related to latent heat release and explained, at least to some extent, as a consequence of the strong reduction of the effective stratification in cloudy regions and, in cases of persistent precipitation into dry air, of low level evaporative cooling [10]. Another consequence of the introduction of humidity is the significant reduction in the intensity of the mountain-induced wind perturbations with respect to dry simulations. A systematic analysis of the upstream flow patterns has been carried out (see [6]) as a function of H, the adimensional height of the mountain, that is the rate between the maximum height of the mountain $h_{\max}$ and the vertical wavelength of dry gravity waves U/N, where U is the typical upstream wind speed and N the dry Brunt-Väisäla frequency. The most interesting features result for values of H corresponding to nonlinear flow regimes, where the formation of upstream blocked areas and the appearance of wave breaking are observed in dry conditions. The occurrence of such features in moist cases is shifted to heights of the obstacle significantly larger than the corresponding values in dry cases, or is completely suppressed [6, 8]. In general, it turns out that the drag is strongly reduced in comparison with the dry case.

The effect of humidity in stationary or nearly stationary conditions is the main subject of the above studies. An accurate analysis of the simulations described in such studies has suggested to carry out a deeper investigation of some properties of the flow that have not been examined in detail so far. In particular, in the present paper attention is mainly devoted to the time evolution of orographic moist flows in non-linear regimes.

In this work, the existence of multiple regimes that may be encountered for particular stages of evolution of the system, possibly associated with the presence of bifurcations [11], will be explored numerically. More generally, we are interested in solutions that, even though transitional, represent "quasi-equilibrium" states, slowly evolving in time as a function of the history of the system. In other terms, we intend to verify the hypothesis that different solutions can be found for the same set of values in the parameter space, if the parameters that control the physical nature of the solution are externally modified in different ways. If this hypothesis is verified, then the resulting flow regime may differ significantly from the regime defined as the final stationary solution obtained in experiments made without changing the inflow conditions and the external parameters during the evolution of the system. The latter type of solutions will be referred to hereafter as "reference" solutions.

For a dry atmosphere, the possibility of obtaining multiple solutions has been shown by [3]. This study has demonstrated that the flow features at the final time can be influenced by the path followed in the parameter space. In the experiments discussed in [3], the value of the (uniform) wind speed at the entrance of the channel has been slowly reduced in time. Once the threshold for wave breaking is exceeded, the curves describing the extremes of wind speed begin to diverge among experiments made with different rates of deceleration, given the same final set of physical parameters. Solutions show up important deviations among the different experiments.

In the present work, we analyse particular paths in the parameter space. The parameters that control the physical nature of the solutions are externally modified by implementing various methods, as described below. Our interest is mainly devoted to the study of the properties of the solutions upstream and near the obstacle.

The mesoscale numerical model BOLAM3 (Bologna Limited Area Model, version 3), the same used in [6], has been employed in a channel configuration. The numerical experiments that have been made with this model describe moist flows over obstacles having different shapes and heights. The results of such simulations are presented here in order to analyse the transient development of the flow field.

In the first set of experiments, the height of the mountain has been modified periodically in the course of the simulations. Our purpose in this case is to verify if the differences in vertical motions and in the consequent extension of condensed areas produced by the enhancement of the mountain height can induce a dependence on the system history, *i.e.* a significant "memory" in the evolution of the system. If this turns out to be true, flow patterns in the initial and final states should differ, although the set of physical parameters is the same at both times.

Subsequently, we have studied, in two distinct sets of experiments, the effect of the progressive increase of humidity inside the model domain. The humidity variations are inserted through a relaxation term added to the equation of evolution of moisture in the first case, and through the advection of moist air from the entrance of the channel towards the mountain (which is initially embedded in dry air) in the second case.

The problem has been studied not only for circular-shaped horizontal cross-section, but also as a function of different mountain geometry. In particular, significant results are obtained for elliptical mountains, with their longer axis perpendicular to the main flow. Such a shape favours the upstream blocking in dry cases. Furthermore, it is shown that the presence of upstream flow reversal helps in maintaining the fore-mountain region separated from the rest of the flow. Therefore, the formation of multiple solutions is favoured.

2. – Model characteristics and numerical setup of the experiments

The numerical and physical setup is very similar to that described in [6]. A channel version of the BOLAM3, a mesoscale model developed mainly at CNR-ISAO [9, 12, 13], has been employed. For the present purpose, we still consider idealised, non-rotating conditions. Model dynamics are based on hydrostatic primitive equations, where the dependent variables are along-channel (longitudinal) and across-channel (latitudinal) wind components (u and v), potential temperature θ, specific humidity q and surface pressure p_s, plus five different hydrometeors. Variables are distributed vertically on a non-uniform, staggered Lorenz grid. The equations are written in a σ-coordinate formulation, with 35 levels. Level spacing is chosen in order to assure a better resolution closer to the ground. The horizontal discretisation is based on an Arakawa C-grid. The horizontal distance between adiacent points carrying the same variable is equal to 15 km. A second-order horizontal and vertical differencing has been employed. A second-order, forward-backward 3D advective scheme [14] and a split-explicit time scheme, with forward-backward integration of gravity waves, have been implemented. The value of the time step is 120 s, with 30 s for the integration of the gravity mode. Free slip conditions are assumed at the surface; however, the presence of internal diffusion makes the flow not completely inviscid. In fact, a fourth-order horizontal diffusion term is added to the prognostic equations, except for the tendency of surface pressure. A second-order divergence diffusion

is included too, more effectively within a sponge layer designed to damp the upward propagating wave energy [15]. For this purpose, the divergence damping is used with a modulated coefficient, increasing slowly with height (see [6] for details). No additional physical processes (surface fluxes, radiation, convection) are implemented in the model version employed here. However, a dry adiabatic adjustment is included in order to produce a gradual adjustment of θ to neutral profile in the case of super-adiabatic conditions that can be produced in regions of gravity wave breaking. An explicit representation of cloud microphysics has been employed, since humid effects are important for our purposes. A parameterisation of the most relevant microphysical processes is included in terms of the local thermodynamic variables in a way similar, for many aspects, to the NEM scheme proposed in [16].

Previous use of the same model for mountain airflow research is reported in [6] and [17]. An extensive description of some preliminary tests, related to the effect of internal model dissipation, horizontal resolution, use of periodic conditions at the entrance and at the end of the channel, conservation of some integral properties and comparisons with results available in the literature are found there.

The dependence of the solutions on the extension of the channel has been studied in some preliminary tests. Spurious reflections at the entrance and at the end of the channel can produce perturbations in the flow. A relaxation scheme [18] has been used to absorb such perturbations. An external border of 8 grid points is used to match the internal fields to the external constant values. However, perturbations may feed back on the internal solutions over relatively long times as those considered here, affecting the flow in a significant way. Tests have shown the necessity of employing a relatively long and wide channel. We used 179×103 grid points in the longitudinal and latitudinal direction, corresponding respectively to 2670×1530 km, for a grid distance of 15 km.

At variance with respect to the simulation strategy reported in [6], where the external parameters controlling the flow are kept constant during the whole simulation, in the present study they are allowed to change during the integration, as specified below, requiring a continuous adjustment of the solutions approaching near equilibrium conditions. Therefore, longer simulations are needed than those employed in [6], in order to obtain stationary or quasi-stationary conditions.

The initial values of the parameters are defined through analytical relationships that calculate 3D fields on the model grid, using pressure as vertical coordinate, before interpolating to sigma coordinates. The initial flow ($U_0 = 10\,\mathrm{m/s}$, $V_0 = 0$) is prescribed uniform inside the channel by an impulsive start-up of the wind, that is defined directly on sigma levels so that the perturbations due to the initial presence of the mountain are reduced. We have verified that such initial perturbations do not affect the long-term evolution of the solutions. Dry Brunt-Väisäla frequency ($N = 0.0134\,\mathrm{s}^{-1}$), surface temperature ($T_\mathrm{s} = 19\,^\circ\mathrm{C}$), mean sea level pressure ($p_\mathrm{s} = 1013\,\mathrm{hPa}$) are prescribed as initial conditions. Values are chosen in such a way that the atmosphere remains convectively stable, though close to neutrality, both upstream and over the obstacle, for the cases considered here, that is with upstream relative humidity $rh \leq 98\%$. Relative humidity is distributed uniformly up to the tropopause, that is located at 150 hPa. In the stratosphere the air is prescribed to be dry ($rh = 1\%$) and the stratification to be larger than in the troposphere ($N = 0.02\,\mathrm{s}^{-1}$).

As will be explained later on, the values of the adimensional height H, at the beginning and at the end of simulations, correspond to different flow regimes in "reference" simulations.

The prescribed orography is Gaussian:

$$h = h_{\max} \exp\left[- \left(\frac{x}{L_x} \right)^2 - \left(\frac{y}{L_y} \right)^2 \right]. \tag{1}$$

In general, the characteristic lengths of the mountain have been fixed to $L_x = L_y = 50\,\mathrm{km}$ for the circular obstacle, and $L_x = 50\,\mathrm{km}$, $L_y = 150\,\mathrm{km}$ for the elliptical mountain. In the range of scales between 10 and 100 km, the flow properties are relatively insensitive to the mountain width. These mountain shapes, although they do not have the simple analytical properties of the bell-shaped mountain [19], have already been studied in detail [20, 21].

3. – First set of experiments: variations of H

The technique we use in the first set of experiments is similar, to some extent, to that employed by [3] in dry simulations. However, in place of using the strategy of deceleration for U_0, we change the height of the mountain in order to modify the adimensional height H (defined in sect. **1**) gradually. This procedure is intended only as one of the possible ways to test the sensitivity of the system to changes in external parameters, in particular to H (or, equivalently, the Froude number) that controls the dry flow dynamics.

In our simulations, the flow is moist and the humidity inflow is constant and close to saturation in the lower-mid troposphere, for each shape of the mountain that has been considered here. We expect that the non-linear effects due to condensation produce non-reversibility in the evolution of the system. In order to verify such hypothesis, the "final" quasi-stationary solution has been compared with the "reference" solution (in the sense defined in the introduction) for the same set of parameters.

At the beginning, simulations have been made with a Gaussian-shaped mountain having a circular horizontal cross-section, and the characteristic length has been fixed to 50 km. The value of relative humidity ($rh = 95\%$) is chosen so that the maximum height of the mountain ($H = 4.0$) gives an upstream blocked moist solution, corresponding to a pronounced lateral deflection ("flow around"), while an unblocked solution, corresponding to a weak lateral deflection ("flow over"), results for the initial and the final value of H ($H = 2.0$). In this way, if there are no multiple solutions, the flow should undergo two symmetric changes of regime. In contrast, if multiple solutions exist, these would result from possible differences emerging between the initial and final regimes of flow, as explained below.

For a Gaussian-shaped mountain, the solution observed after the height of the obstacle has been modified according to the path described in fig. 1 does not present significant differences with the "reference" solution obtained for $H = 2.0$. The variation in the intensity of the upstream minimum of the zonal velocity component U with H is shown in fig. 2. The time evolution of the point representing the state of the system is clockwise along the curve. The area delimited in the parameter space reveals the presence of a "hysteresis cycle", indicating the existence of a short-term "memory". However, this behaviour may be due to the fact that the fluid does not adjust instantaneously to the changing height of the mountain: therefore, the flow is not representative, during the evolution, of the "reference" steady state based on the height of the obstacle at the same instant. At the end of the simulation (fig. 3), no significant differences can be observed between values of U of the solution obtained at the end of the path in fig. 1 and the corresponding "reference" solution (4.4 m/s).

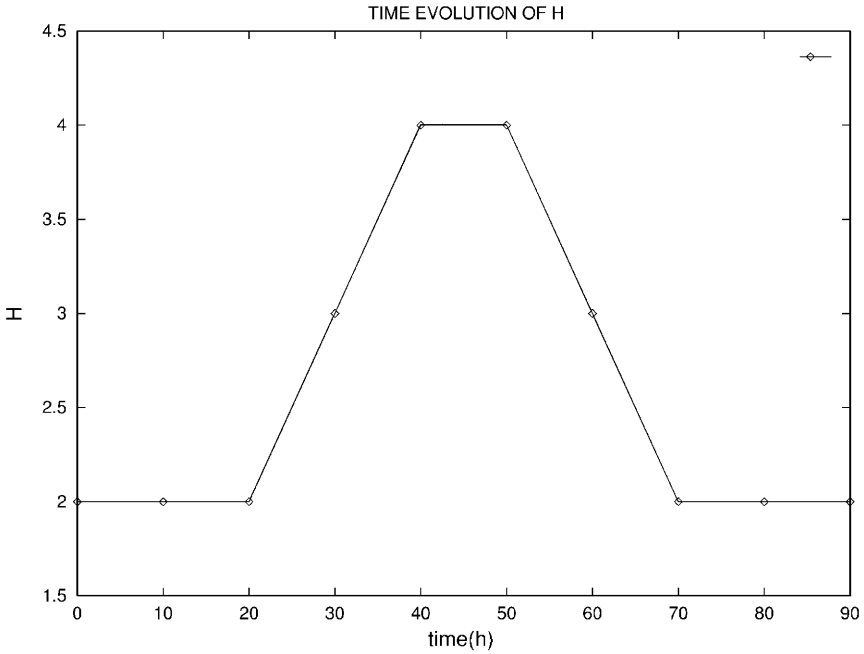

Fig. 1. – First set of experiments: time evolution of H during the simulation for the circular-shaped mountain.

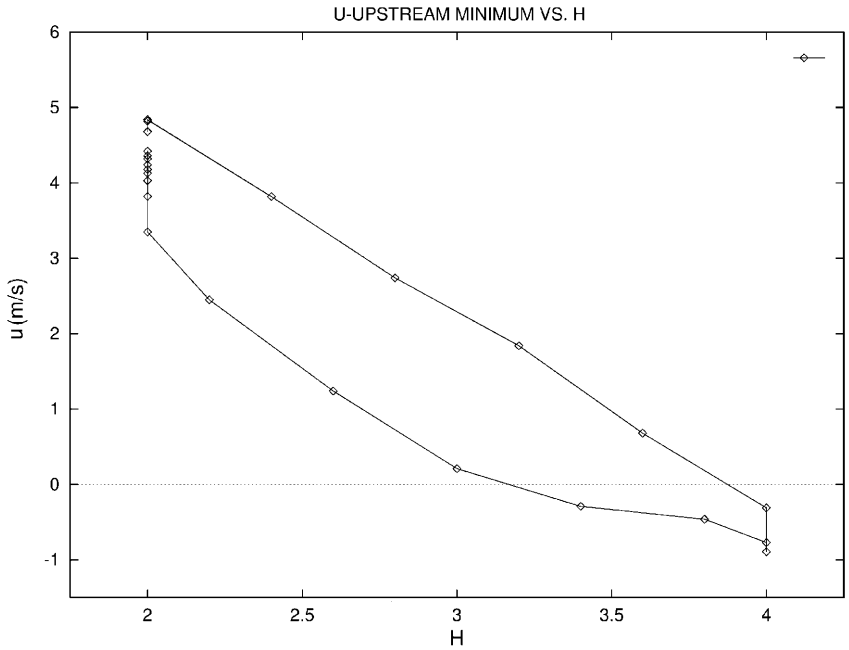

Fig. 2. – First set of experiments, circular mountain: intensity of the upstream minimum of u component of velocity *vs.* H. The point, representing the state of the system, moves clockwise with time on the curve. Each diamond represents values at 4 hour intervals.

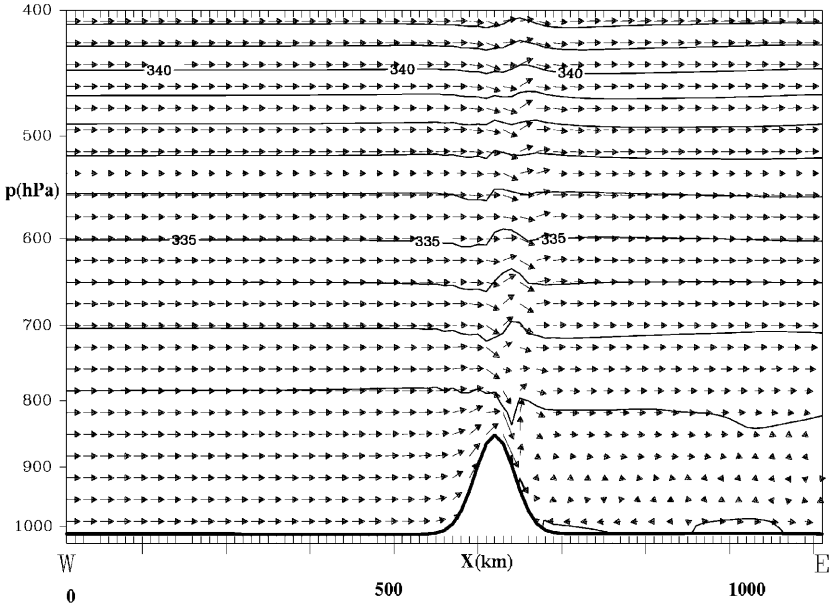

Fig. 3. – First set of experiments, circular mountain: vertical cross-section of equivalent potential temperature and wind vectors (u and w components) along the central axis of the channel at the end. The contour interval is 1.0 K.

Then, we repeated the above experiments with an elliptical Gaussian mountain, having a longitudinal characteristic length of 50 km and an aspect ratio of the north-south to east-west length greater than 1 (in this case equal to 3). Smolarkiewicz and Rotunno [22] and Bauer *et al.* [21] demonstrated that, in dry conditions, the upstream reversal extends progressively upstream as the section of the mountain transversal to the flow increases.

The path of evolution of the height of the mountain is the same prescribed for the circular obstacle, shown in fig. 1. For the value of relative humidity considered ($rh = 95\%$), a regime of "flow over", but very close to upstream stagnation, characterizes the "reference" solution for the initial value of H ($H = 2.0$). A regime of "flow around" characterizes the "reference" solution for the maximum value of the obstacle ($H = 4.0$).

For the elliptical obstacle, a significant difference at the end of the simulation can be observed in the intensity of the upstream minimum of the zonal component of velocity (1.8 m/s after 90 h) with respect to the value (2.8 m/s) reached after 20 hours of integration. Therefore, the change of H produces a decrease in the value of the upstream minimum. In order to better understand the above result, cross-sections along the central axis of the channel, depicting the solutions after 20 hours ($H = 2.0$), 40 hours ($H = 4.0$) and 90 hours ($H = 2.0$), respectively, are shown in fig. 4. In particular, fig. 4a represents the quasi-equilibrium flow regime (the solution is not totally stationary in this case) of the "reference" solution for the initial mountain height, while fig. 4c depicts the final state for the same orography after the evolution of the system has been completed. Figure 4b is representative of a quasi-steady solution for the case of a high mountain. The initial regime of "flow over" (fig. 4a) gradually changes into a partly blocked regime as the height of the mountain is varied and reaches its maximum. A (small) portion of the air located near the ground, immediately upstream of the obstacle, does not flow

over it any longer, after the flow has adjusted to the high value of H corresponding to a regime of "flow around", even in the moist case. No condensation occurs in this case at low levels upstream of the mountain and a relatively low amount of humidity is present there, associated with a weak downward motion (the presence of sinking upstream is a general characteristic of the blocked flow, see for instance [1] and [22]). The equivalent potential temperature θ_e, immediately upstream of the obstacle (fig. 4b), decreases after 20 h (fig. 4a). Once the value of H is then lowered to its initial value ($H = 2.0$), the flow upstream and over the obstacle does not totally recover the features characterising

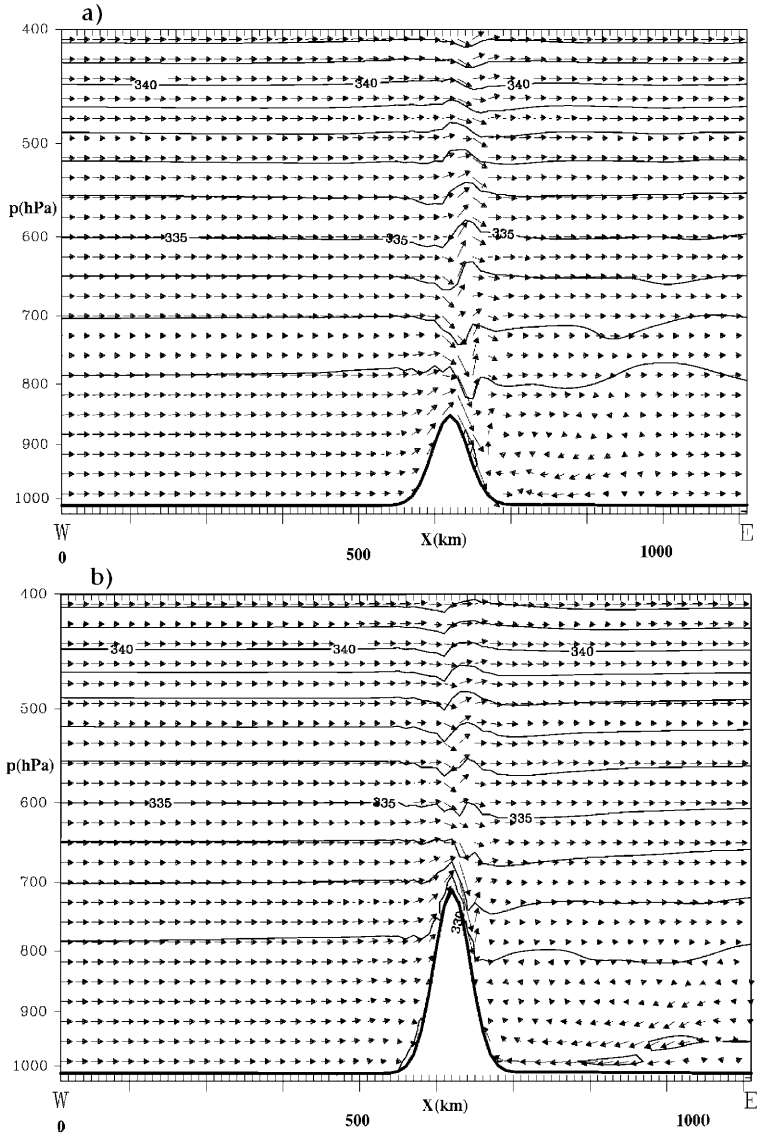

Fig. 4. – As fig. 3, but for an elliptical mountain, after 20 hours (a), after 40 hours (b) and after 90 hours (c).

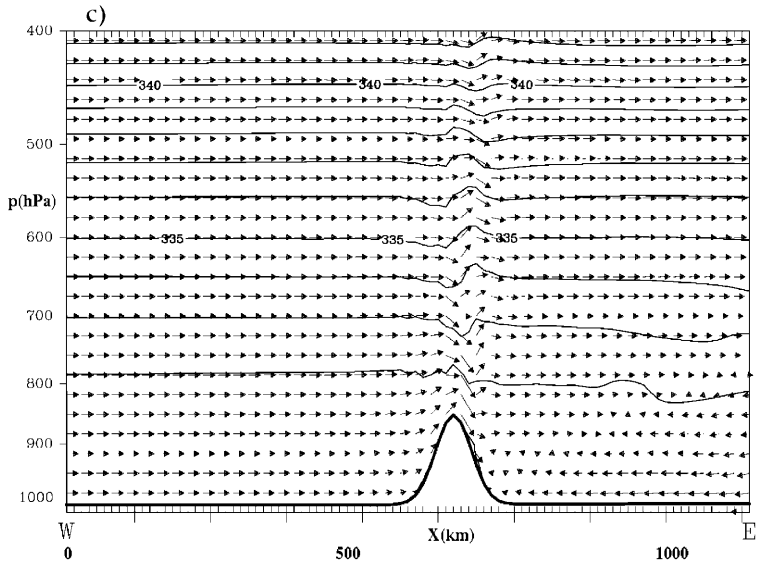

Fig. 4. – Continued.

the state of fig. 4a. The reduction of vertical motion, characterising the flow upstream for $H = 4.0$ and associated with a reduction in the latent heat release, persists, to some extent, also in the final state for $H = 2.0$. This is consistent also with the cloud water content immediately over the mountain and with the local maximum of precipitation rates, which presents values smaller than after 20 h (not shown), similar to those observed for $H = 4.0$.

The comparison of the results obtained with different shapes of the obstacle indicates that the shape of the mountain is really important and, indirectly, reveals that the extension of blocked and/or reversed flow upstream is the main factor that favours the manifestation of multiple solutions. The choice of an intermediate flow regime with a strong upstream reversed flow is related to the purpose of obtaining a region separated from the rest of the flow. In regions of closed circulation, the materially conserved properties along the streamlines, as potential vorticity or humidity in the absence of condensation, may differ from those in an open flow. For our purposes, the most interesting regions of separated circulation are those upstream. The presence of upstream closed circulation may be associated in principle with multiple solutions, if these regions maintain their identity while the system is moved toward points in the parameter space normally deprived of such flow patterns.

In the simulations described in this section, a "flow over" type of (moist) solution, that establishes itself as a result of a transition from a blocked flow regime, appears to be different from a solution for the same parameters that is established in the absence of such previous blocked flow. In the first case, the solution still "remembers" some aspects of the blocked flow, in the sense that the rising motion upstream, and the associated release of latent heat, are smaller than in the latter case, and the differences are more evident for a mountain that favours the formation of blocking. For example, in the case of the circular mountain, simulations (not shown) indicate that the upstream volume of low θ_e moves downstream more quickly than for the elliptical-shaped mountain. With

respect to the "reference" solutions, the structure of the flow features does not change in the case of a circular mountain, whereas more significant differences appear in the case of an elliptical mountain.

The solutions described in this subsection are not completely stationary, especially for the case of an elliptical mountain; therefore, we cannot exclude that, for a longer time interval, the system tends, even very slowly, to the "reference" values. Nevertheless, we think that the time interval considered here is long enough, if compared with the typical transitional time of evolution towards stationary solutions, to consider these results as physically meaningful.

4. – Second set of experiments: humidity source

In this second attempt of investigating the effects of humidity on the system properties, starting conditions are chosen once again so that an initial upstream blocking is present. No condensation is allowed at the beginning ($rh = 50\%$), but the parameter values, namely H, are chosen in such a way that they correspond to a "flow over" regime in the case of moist flows, as specified below. In this case, the height of the mountain is kept constant in time. After 20 hours, during which a regime of "flow around" is established (independently of the particular shape of the obstacle), moisture is added everywhere inside the channel in a progressive way. At each time step, a term proportional to the deviation from a prescribed value of specific humidity (defined as a corresponding relative humidity, in the troposphere, of 98% for the circular mountain, 97% for the elliptical mountain) is inserted into the equation of evolution of specific humidity, with a characteristic relaxation e-folding time of 5 hours. The choice of the reference value of humidity is a subtle subject. A value of 100% is of course the upper limit, and would produce condensation for upward motion, no matter how small, and therefore would lead to unrealistically large condensed volumes. Too small a value, in contrast, may prevent saturation in regions of ascent that otherwise would be saturated, and then could hinder the dynamical effects of condensation we are interested in. A long relaxation time, as the one chosen here, allows for the persistence of condensation in areas of strong enough vertical motion also for relative humidity equal to 97–98%.

The first case considered here is again that of a Gaussian obstacle, with a circular horizontal cross-section. We chose a value of $H = 2.5$ corresponding to the strongest reversed flow in the dry simulations, but to "flow over" in the corresponding moist case with relative humidity equal to 98%, as shown in [6]. The choice, as initial condition, of a regime with a strong upstream reversed flow is related to the possibility of obtaining a region separated from the rest of the flow. The solution, after the period of "moistening" (lasting for 16 hours), evolves from the initial "flow around" towards the "reference" moist solution in about 25–30 hours. The flow features are qualitatively the same; however, a clear difference with respect to the reference solution can be found in the intensity of the upstream minimum at the end of the simulations (4.8 m/s *vs.* 5.6 m/s).

The second case is, as in the previous section, that of an elongated elliptical mountain, which emphasises the effect of the upstream blocking. The choice of the height ($H = 3.0$) and of the final relative humidity ($rh = 97\%$) corresponds to the same criteria considered for the circular mountain. The results show clearly the presence, during the simulation, of a flow regime completely different from the "reference" one. Figure 5 illustrates the evolution of the solution compared with the reference moist case. The upstream minimum of the u component remains negative during almost the whole time of the simulation (110 hours), and even when, at the end, it becomes positive, it remains much smaller

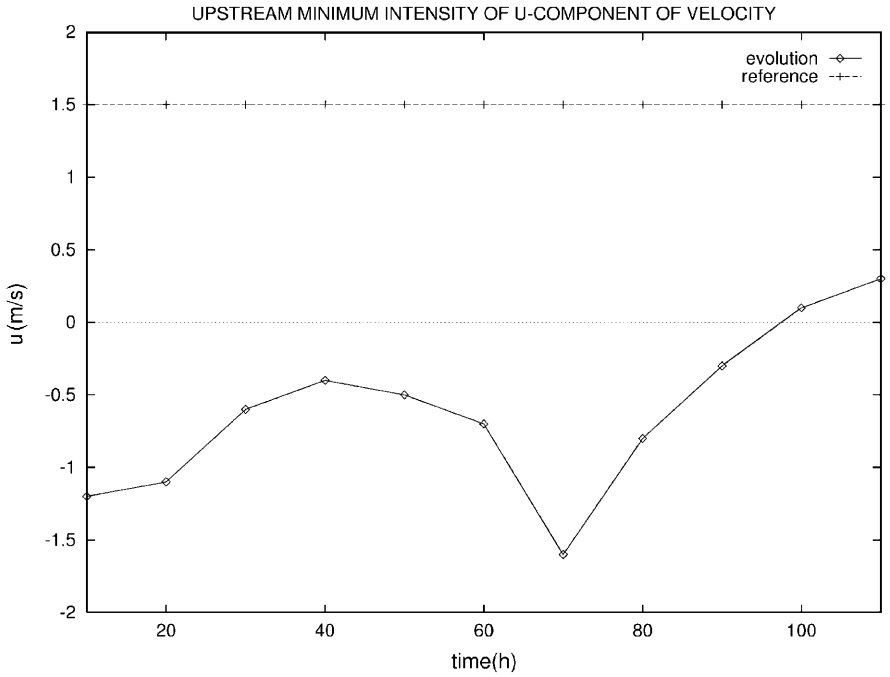

Fig. 5. – Second set of experiments, elliptical mountain: upstream u-component minimum *vs.* time, compared with the "reference" moist solution.

than the "reference" value. In order to test the sensitivity of the final flow characteristics to the imposed humidity changes, simulations with doubled e-folding time of relaxation of humidity have been performed. However, the same significant flow changes, with respect to the reference case, have been observed.

An analysis of the solution shows that the elongated shape of the mountain favours the persistence of a dry region immediately upstream of the obstacle. A wide area of low equivalent potential temperature (fig. 6) and a strong reversed flow persist upstream longer than in the case of a circularly symmetric mountain, where the dry air flows around the obstacle quickly. In the lowest levels, the immediately upstream circulation moves the air downward along the windward slope, partially drying it. Therefore, due to the downward motion, dry air remains confined upstream in spite of the moistening relaxation term, while moist air in the upper levels moves upward and condenses. The horizontal maximum extension of the reversed flow corresponds to the appearance of saturated portions near the obstacle (about 60 hours after the initial time), that limit the drier air to a shallow layer and push it downward. Later during the experiment, the horizontal extension of the upstream dry portion is reduced, but at the end, though small, it tends to remain almost stationary. Figure 7 shows the wind vectors at the lowest sigma. The presence of an evident low-level "flow around" can be distinguished upstream and aside of the obstacle. Therefore the blocking, favoured by the particular shape of the mountain, can really modify the evolution of the flow in this particular system. In contrast with the results of the first set of experiments, the upstream drier region persists detached from the rest of flow until the end of the simulation.

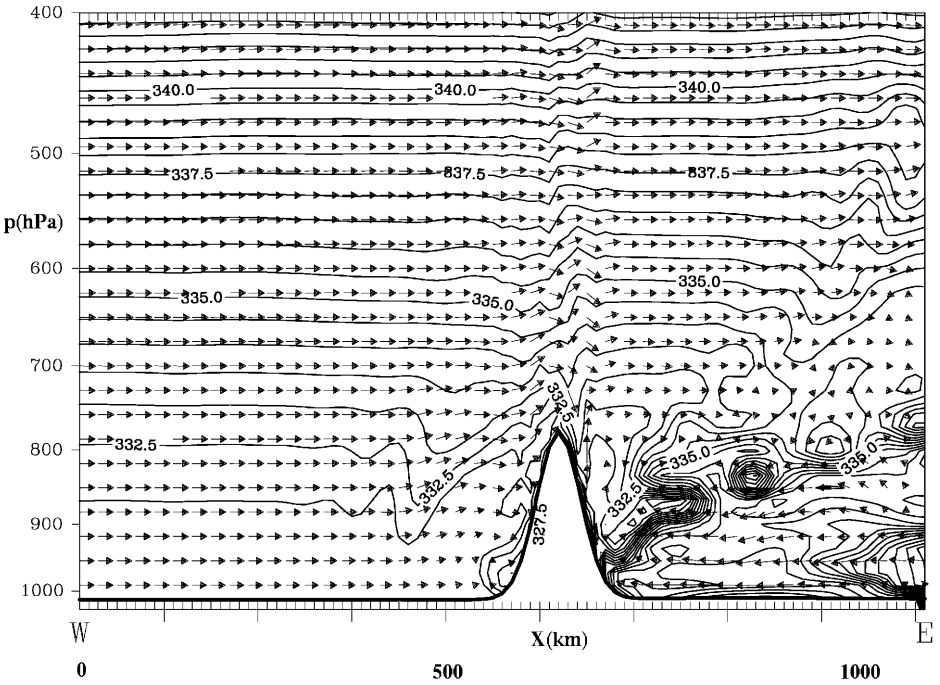

Fig. 6. – As fig. 4, but for the second set of experiments, after 60 hours. The contour interval is 0.5 K.

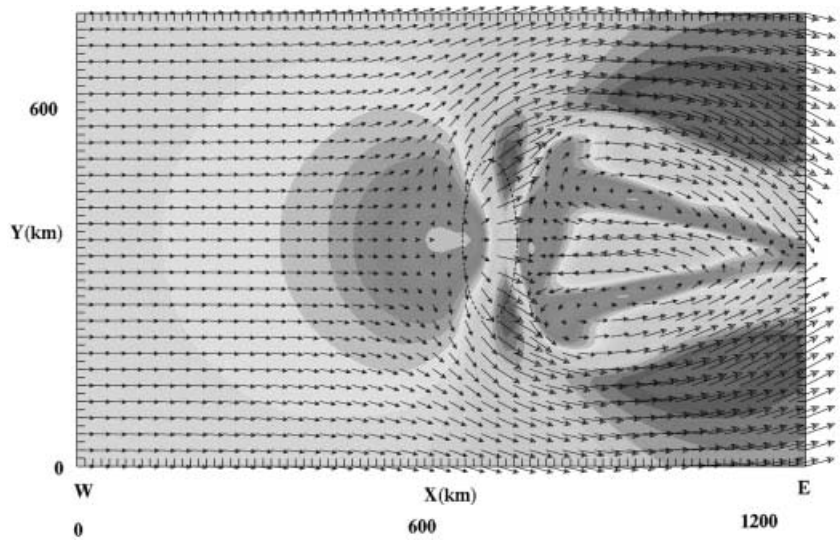

Fig. 7. – Second set of experiments, elliptical mountain: wind vectors at the lowest model level (about 20 m), after 60 hours.

In order to test once again the sensitivity of the flow evolution to the presence of blocking, additional experiments have been made in the case of a boomerang-shaped mountain, with its concave side facing upstream. This shape favours the formation of a stronger and wider flow reversal than for the other mountain shapes considered here. For the kind of evolution described in this section, the reversal persists for this particular mountain shape until the end of the experiments, and the intensity of the upstream minimum is stationary at the end. The features obtained for the elliptical case are emphasised by this new shape, as a consequence of the stronger blocked flow.

5. – Third set of experiments: advection of moisture

In the last series of experiments, a more realistic situation has been considered. In this case, the advection of moist air from the entrance of the channel toward an obstacle, initially embedded in dry air, determines a transition from dry to humid conditions. The transitional zone between the pre-existing dry air and the incoming moist air advances as a sort of "humidity front".

The initial condition is chosen in such a way that the troposphere is divided into two different volumes: a moist region ($rh = 98\%$) occupies the first upstream 300 km, and a dry region ($rh = 1\%$) the rest of the channel. A humidity constant gradient is defined in a region 75 km wide, making the transition between the two different regions smooth. The temperature distribution is defined initially in such a way that values of virtual temperature on each level are the same in moist and dry regions. This definition avoids the generation of horizontal density gradients due to moisture gradients, that would impose a solenoidal forcing and hence would alter the flow dynamics with respect to the case with uniform humidity. In this way, the "humidity front", characterised by a weak temperature gradient (at the beginning, the moist air is about 2 degrees cooler at the surface than the dry air) can preserve its vertically coherent structure before its arrival over the obstacle.

An alternative, though less physical approach, has been tested in order to avoid unwanted baroclinic effects along the "humidity front". In this case, the model definition of virtual temperature has been altered simply by setting it equal to the absolute temperature. Tests have shown the same qualitative flow patterns as in the first approach.

As in the previous experiments, the initial set of parameters corresponds to a regime of "flow around" in a dry atmosphere. In order to obtain an accurate comparison of the role of different mountain shapes for the procedure discussed in this section, obstacles having the same height ($H = 3.0$) have been studied for the circular and the elliptical cases.

A circular-shaped mountain with $L = 50$ km presents a regime of "flow over" just 20 hours after the passage of the front (40 hours after the beginning of the simulation). However, a significant difference in the upstream u-wind component minimum appears with respect to the "reference" moist solution (2.4 m/s *vs.* 4.6 m/s). Fourty hours after the passage of the frontal system, most of the pre-existing dry air has moved downstream and no blocking can be found: in this case, the intensity of the upstream wind component near the central axis of the channel is stronger than for the elliptical mountain. In contrast, for a wider circular obstacle, having the radius equal to the transversal characteristic length of the elliptical mountain ($L = 150$ km), after 40 hours the region of reversal is still wide. In particular, an extensive region of confluence of reversed flow with the main current appears far upstream of the mountain (fig. 8a). However, also in this case the upstream minimum becomes positive after 70 hours. Figure 8b shows the flow pattern after 80 hours.

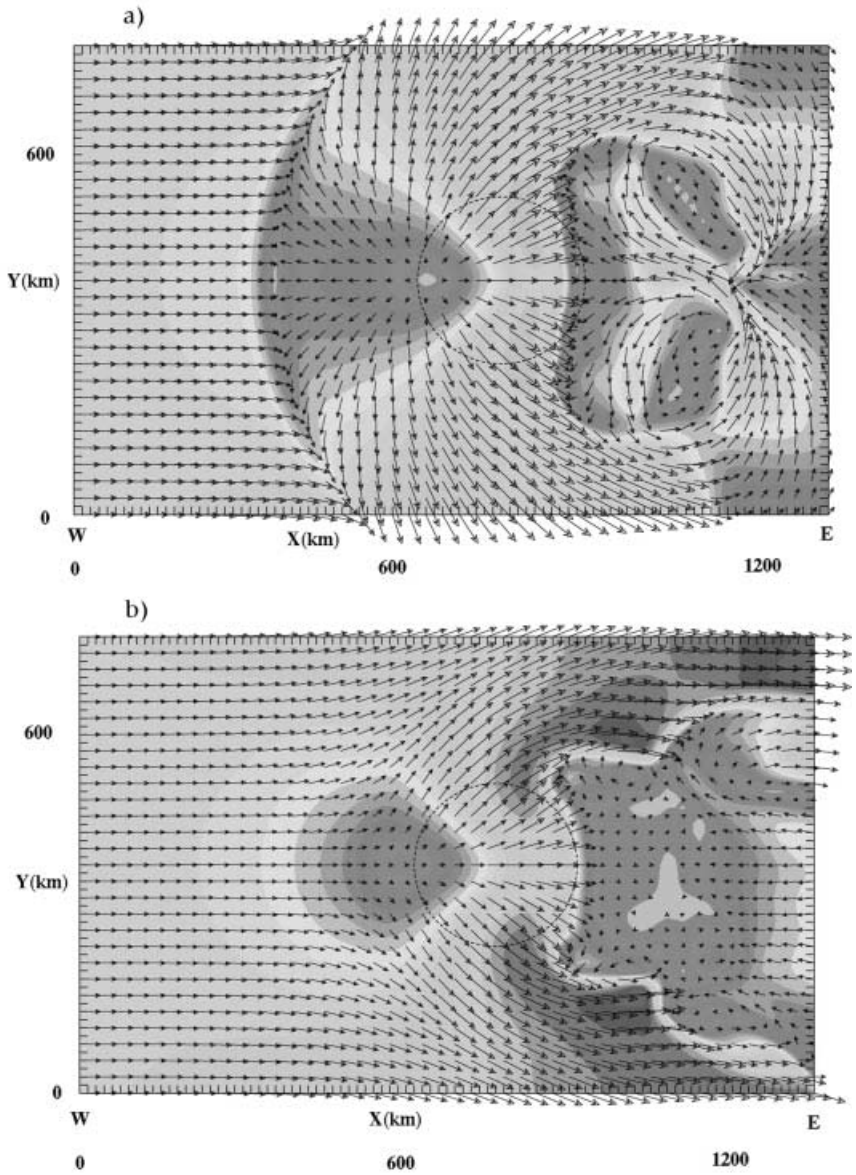

Fig. 8. – Third set of experiments, circular mountain ($L_y = 150$ km): wind vectors at the lowest model level, after 40 hours (a) and 80 hours (b).

For an elliptical obstacle blocked flow features persist until the end of the simulation (100 hours), even in the region of parameter space corresponding to "flow over" in "reference" moist solutions. After 80 hours (60 hours after the arrival of moist air over the obstacle), a reversed flow affects the region immediately upstream of the obstacle (fig. 9). So, not only the aspect ratio and the adimensional height, but also the obstacle geometry are important in determining the evolution of the system.

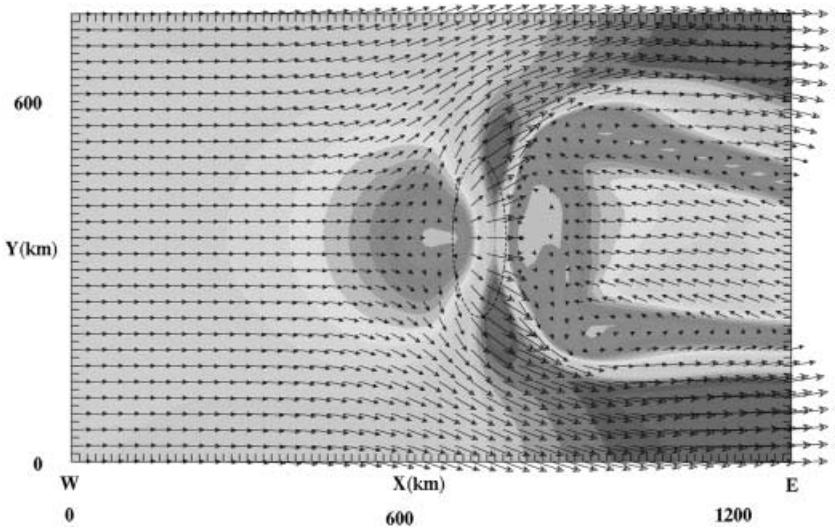

Fig. 9. – Third set of experiments, elliptical mountain: wind vectors at the lowest model level, after 80 hours.

In the remaining of this subsection, an interpretation of flow features will be given for the elliptical mountain. A comparison is made among the "reference" moist solution (fig. 10a), the advective moist solution (fig. 10b), attained immediately after the advection of moist air over the obstacle has taken place, and the dry solution (fig. 10c): all of them are shown 40 hours after the beginning. While in the "reference" moist case a "flow over" regime can be observed, the advective solution after the passage of the "humidity front" over the obstacle still presents a wide portion of reversed flow, even larger than in the dry solution. This area is bounded on the upwind side by a strong horizontal wind shear in the region of confluence between direct and reversed flows.

The differential advection, generated by the vertical shear induced by the mountain, modifies the "humidity front" in a strong way (see also the patterns observed in [23-25], and the theoretical calculations in [19]). Near the ground the incoming flow is slowed down, while at upper levels the moist air moves more rapidly. The convergence and the lifting ahead of the barrier get the incoming moist air condensing far upstream: the decoupled upstream region behaves as an "extension of the mountain for orographic lift purposes" [26]. An extended upstream cloud is generated, with two regions of maximum water content (fig. 11). The first one is located immediately upstream of the obstacle and corresponds to the typical uplift generally observed close to the mountain. The second one is the consequence of the rising of air far upwind of the obstacle and is due to the low-level convergence bordering the blocked area, resulting in precipitation also far upstream (see also [27]). During the simulation, when the extension of the drier blocked air is progressively reduced, also the second upstream cloud decreases by retreating towards the ground and towards the mountain. The moist air following the humidity front flows more quickly around the obstacle than along the central axis. The deformation of the front induced by the mountain leaves a wide drier volume of air upstream of the mountain. The transfer of a reduced amount of moisture into the separated region and the consequent downward vertical motion prevents the occurrence of condensation in such region (see again fig. 11).

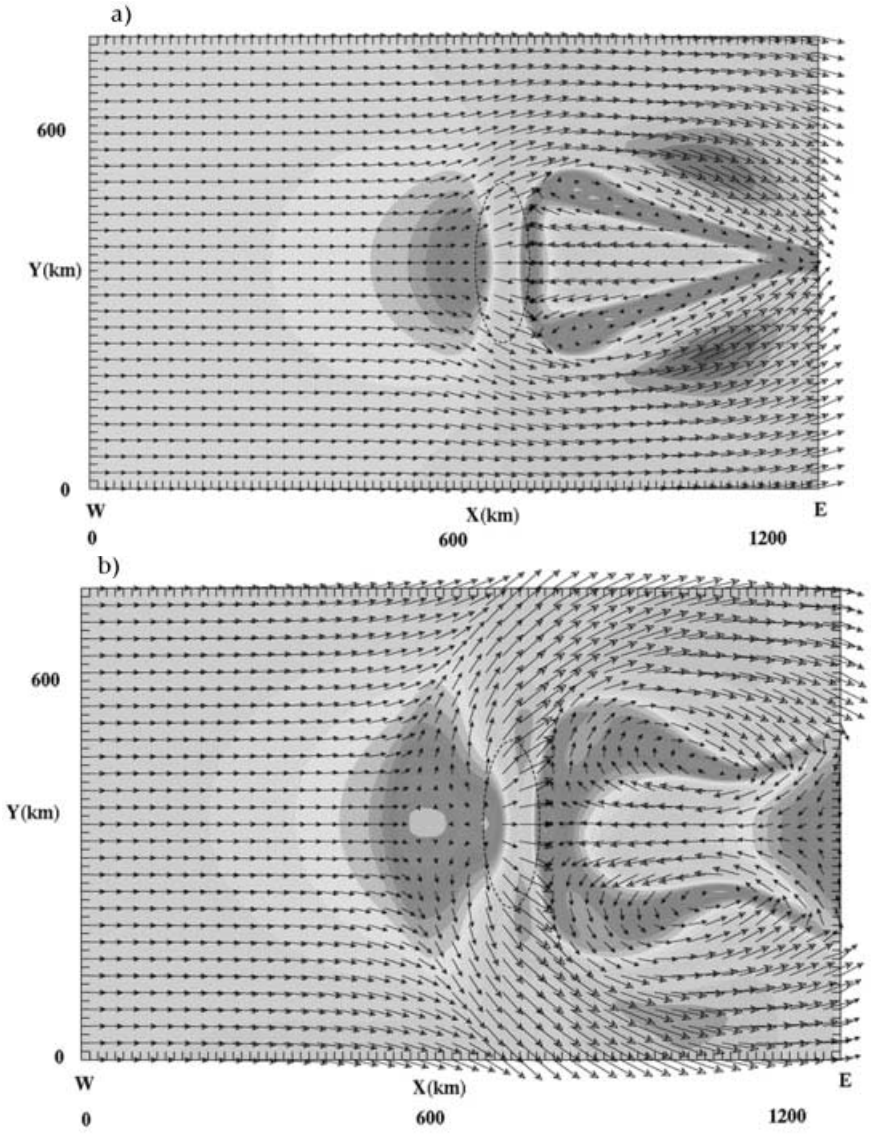

Fig. 10. – Elliptical mountain: wind vectors at the lowest model level, in the "reference" moist case (a), in the third set of experiments (b), in the "reference" dry case (c). All the figures are after 40 hours.

A vertical cross-section through the central axis of the channel is presented in fig. 12. The region of low θ_e is associated with the upstream minimum of the u-wind component. An interesting evolution regards the upstream flow patterns. Immediately after the impact of the humidity front on the obstacle (about 20 hours), a maximum in the intensity of the flow reversal is observed. Then, this region of reversed flow reduces progressively in the following 40 hours. The extension of this region and the intensity of the minimum (-0.7 m/s) remain almost stationary during the last 40 hours. At the end of the sim-

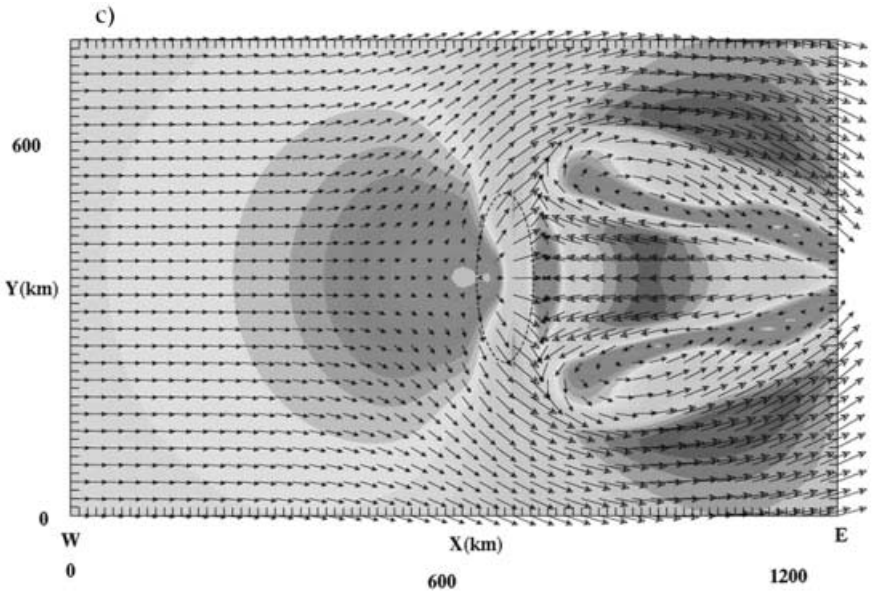

Fig. 10. – Continued.

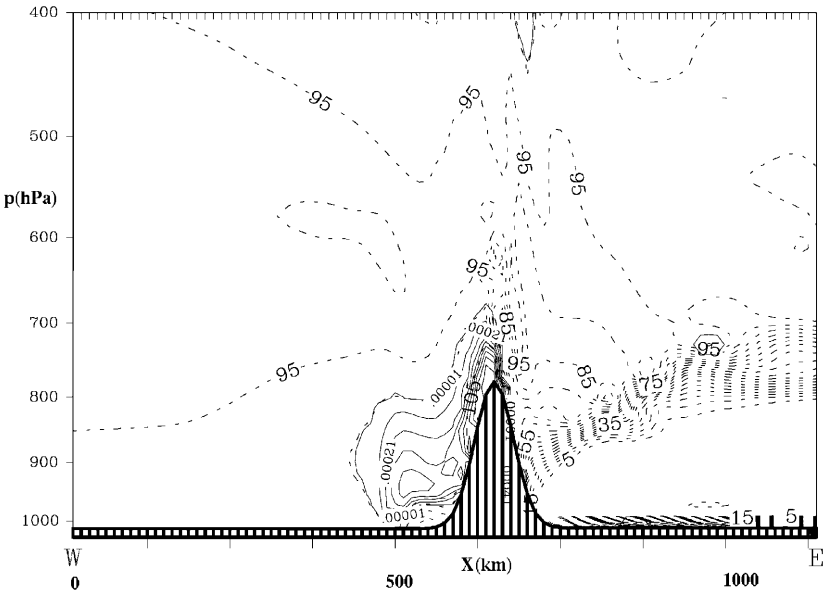

Fig. 11. – Third set of experiments, elliptical mountain: vertical cross-section of liquid water content and of relative humidity along the central axis of the channel, after 40 hours.

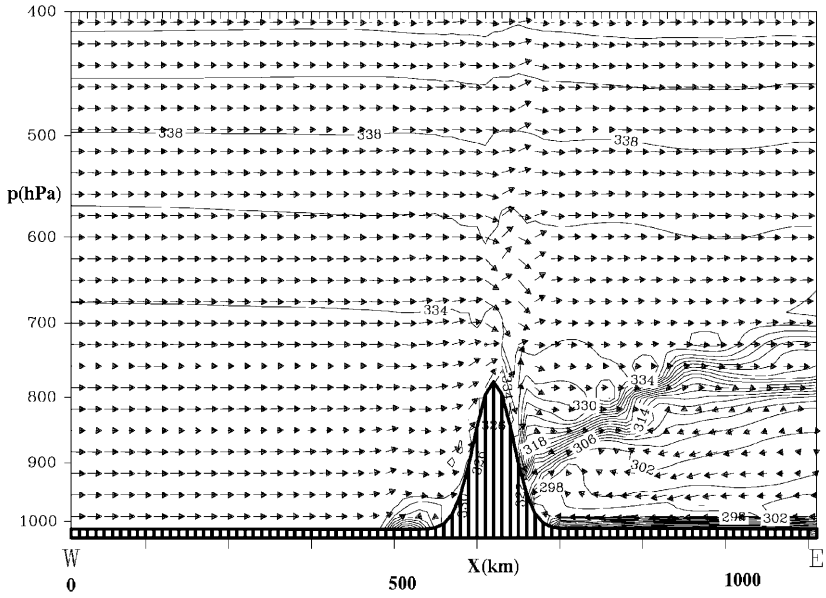

Fig. 12. – As fig. 11, but for equivalent potential temperature and wind vectors after 40 hours.

ulation, a reversal is still present and its horizontal extension remains large. However, its vertical extension, that is several hundred meters deep immediately after the passage of the front, is reduced to only a few hundreds later on. The solution appears almost stationary at the end: the observed evolution time is very long in comparison with the typical time needed by the adjustment toward stationary solutions in simulations with orographic forcing.

In conclusion, a non-trivial solution appears in the experiments described in this subsection. The role that is played by the separated upstream regions turns out to be fundamental in producing evolutions of the flow that are different from the "reference" solutions. The intensity of such features depends on the particular shape of the obstacle. It is interesting to observe that, in these advective simulations, at least for the elliptical obstacle, the presence of humidity even strengthens the upstream blocking with respect to the "reference" dry case.

6. – Discussion and conclusions

This work extends a previous study of stationary solutions in moist flows over simply shaped mountains in idealised atmospheric conditions [6]. The earlier results have suggested an analysis of some aspects of the problem that had not been considered so far. In particular, the possibility of revealing non-stationary solutions and the possible existence of multiple solutions have been investigated in a moist atmosphere. This work can be considered, for some aspects, as aimed at a generalisation of the results obtained in dry conditions [3].

The interpretation of numerical results is not so straightforward. However, in some cases, our simulations have shown solutions whose flow features are different from the "reference" solutions, obtained by considering from the beginning uniform humidity in-

flow and constant flow parameters. Such solutions do not appear simply as an extension of those already found in the dry case, but are specifically related to the effects of condensation (and evaporation in some cases), coupled with those associated with the dynamical properties of flow past an orographic obstacle. The non-linearity due to moist processes depends on the latent heat exchange occurring at the saturation threshold. Such diabatic effects, are responsible for the non-trivial, time-dependent but long-lasting solutions that appear in the numerical simulations of the present study.

The experimental set-up has been guided by hypotheses based on physical considerations of the properties of flow regimes past obstacles and of the effects of humidity on stationary or quasi-stationary solutions [6]. Experiments reveal that it is possible to obtain, by imposing certain types of evolution in the flow parameters, solutions characterised by portions of flow reversal, nearly separated from the rest of the flow. These features occur in regions of the parameter space that lead to different regimes in simulations where the inflow conditions and the external parameters do not change in time. Different solutions have been obtained for different paths and by using different methods, for the same set of parameters. Therefore, the "history" of the system is important in determining different ways of evolution of the atmosphere.

Only a few particular paths in the parameter space, that present the most interesting flow features, have been considered here. In the first set of experiments, the possible existence of multiple solutions for the same set of parameters has been analysed in relation with the role of condensation, associated with the different orographic regimes of "flow over" or "flow around". The evolution of the system has been obtained in this case by changing the height of the mountain in the course of the simulations. The chosen extreme values correspond to different flow regimes. A change in the evolution of the system, even if weak, can be attributed to the non-reversibility associated with condensation. The reason is related to the persistence of an upstream dry region, separated from the main flow, that has been observed to appear for the maximum value of the mountain height.

In the second case considered here, multiple solutions have been found by including, in the equation of evolution of humidity, a forcing term that drives the system from an initial dry atmosphere to a final moist atmosphere. A regime of "flow around" is still present also in the moist case, in contrast with the "reference" moist simulations.

In the third case, a somehow more physical system configuration has been considered. The presence of a slowly evolving, not obvious, time-dependent solution can be distinguished, due to the advection of moist air. Not only a wide region of flow reversal remains confined upstream of the obstacle also after the arrival of moisture, but the intensity of the upstream blocking is, for a long time, even enhanced with respect to the initial dry flow regime. This solution is almost stationary, since the characteristic time of evolution is very long compared to the typical transitional time of evolution toward stationary solutions.

The importance of the shape of the mountain for our results has been demonstrated by comparing solutions obtained for obstacles having different geometry. In particular, interesting solutions appear for elliptical mountains, which favour the persistence of upstream dry regions. In our simulations, these regions are generally associated with upstream closed circulation. Since these regions tend to maintain their identity even if the system parameters are changed, they can be associated with the existence of multiple solutions or, at least, with slow evolution of the flow. This can account for the fact that the initial "flow around" regime partly survives even after moistening of the air. For circular mountains, the system evolves in a shorter time than in the elliptical case.

The results of this work are not to be interpreted as purely theoretical. Analysing the existence of particular non-stationary solutions may serve as a basis for interpreting features actually observed in real events. Appropriate field observations, as those gathered in the context of the Mesoscale Alpine Programme [28], represent a valid reference for further verification of the results described here.

* * *

This work has been partially supported by the CNR (Progetto Strategico MAP) and the European Social Fund (ESF).

REFERENCES

[1] Smolarkiewicz P. K. and Rotunno R., *J. Atmos. Sci.*, **46** (1989) 1154.
[2] Schär C. and Durran D. R., *J. Atmos. Sci.*, **50** (1993) 1373.
[3] Smith R. B. and Grønås S., *Tellus A*, **45** (1993) 28.
[4] Durran D. R. and Klemp J. B., *J. Atmos. Sci.*, **39** (1982) 2490.
[5] Jusem J. C. and Barcilon A., *Geophys. Astrophys. Fluid. Dyn.*, **33** (1985) 129.
[6] Miglietta M. M. and Buzzi A., *Tellus A*, **53A** (2001) 481.
[7] Schneidereit M. and Schär C., *Meteorol. Atmos. Phys.*, **72** (2000) 233.
[8] Jiang Q. and Smith R. B., in *1999 AMS Conference on Mesoscale Meteorology, Boston.*
[9] Buzzi A. and Foschini L., *Meteor. Atmos. Phys.*, **72** (2000) 131.
[10] Durran D. R. and Klemp J. B., *J. Atmos. Sci.*, **39** (1982) 2152.
[11] Guckenheimer J. and Holmes P., *Nonlinear Oscillations, Dynamical Systems, and Bifurcation of Vector Fields* (Springer) 1983.
[12] Buzzi A., Fantini M., Malguzzi P. and Nerozzi P., *Meteorol. Atmos. Phys.*, **53** (1994) 137.
[13] Buzzi A. and Malguzzi P., *MAP Newsletters*, **7** (1997) 98.
[14] Malguzzi P. and Tartaglione N., *Q. J. R. Meteor. Soc.*, **125** (1999) 2291.
[15] Klemp J. B. and Lilly D. K., *J. Atmos. Sci.*, **35** (1978) 78.
[16] Schultz P., *Mon. Weather Rev.*, **123** (1995) 3331.
[17] Miglietta M. M. and Buzzi A., *MAP Newsletter*, **11** (1999) .
[18] Lehmann R., *Meteorol. Atmos. Phys.*, **52** (1993) 1.
[19] Smith R. B., *Mon. Weather Rev.*, **110** (1982) 306.
[20] Bauer M. H., *Three-dimensional numerical simulations of the influence of the horizontal aspect ratio on flow over and around a mesoscale mountain*, PHD thesis (Dept. of Meteorol. and Geophys., University of Innsbruck) 1997.
[21] Bauer M. H., Mayr G. J., Vergeiner I. and Pichler H., *J. Atmos. Sci.*, **57** (2001) 3971.
[22] Smolarkiewicz P. K. and Rotunno R., *J. Atmos. Sci.*, **47** (1990) 1498.
[23] Hobbs P. V., Houze R. Jr. and Matejka T., *J. Atmos. Sci.*, **32** (1975) 1542.
[24] Marwitz J. D., *J. Appl. Meteor.*, **19** (1980) 913.
[25] Heggly M. F. and Reynolds D. W., *J. Climate Appl. Meteor.*, **24** (1985) 1258.
[26] Peterson T. M., Grant L. O., Cotton W. R. and Rogers D. C., *J. Appl. Meteorol.*, **30** (1991) 368.
[27] Grossman R. L. and Durran D. R., *Mon. Weather Rev.*, **112** (1984) 652.
[28] Bougeault P., Binder P., Buzzi A., Dirks R., Houze R. Jr., Kuettner J., Smith R. B., Steinacker R., Volkert H., *Bull. Am. Met. Soc.*, **82** (2001) 433.